Mathematical modeling of plumes impingement on landing site of “ExoMars” landing platform

Anuar Kagenov, Anatoliy Glazunov, Kirill Kostyushin, and Ivan Eremin

Citation: AIP Conference Proceedings **1899**, 060010 (2017);
View online: https://doi.org/10.1063/1.5009881
View Table of Contents: http://aip.scitation.org/toc/apc/1899/1
Published by the American Institute of Physics

Mathematical Modeling of Plumes Impingement on Landing Site of "ExoMars" Landing Platform

Anuar Kagenov[a)], Anatoliy Glazunov[b)], Kirill Kostyushin[c)] and Ivan Eremin[d)]

National Research Tomsk State University, 36 Lenina Avenue, Tomsk, 634050 Russian Federation

[a)]Corresponding author: anuar@ftf.tsu.ru
[b)]gla@niipmm.tsu.ru
[c)]kostushink@hotmail.com
[d)]iveremin@niipmm.tsu.ru

Abstract. This paper presents the results of numerical studies of the interaction of underexpanded four supersonic plumes with surfaces. The final stage of controlled landing of "ExoMars" landing platform on the surface of Mars is considered. The altitude of landing platform from 1 to 0.3 meter above the surface of Mars and the thrust level of the propulsion system is varied. The distributions of the parameters of gas near landing platform are obtained during operation of propulsion system at the minimum and maximum thrust. The ground effect lift loss under Mars conditions for given configuration landing platform is investigated. The insignificant of ground effect lift loss at altitude 1 meter was found and value of lift loss varied from 1 % to 3% depending on level of propulsion system thrust. For another altitudes, received significant effect of external pressure on the bottom surface of landing platform. The magnitude of this external pressure reached 26% of the maximum thrust of propulsion system.

INTRODUCTION

One of the priorities in the study of the planets of the Solar system is the exploration of Mars. This is due to the fact, that Mars relative to other planets has the closest physical characteristics to the Earth. Currently, the exploration of Mars carried out using artificial satellites placed in the orbit, landing platforms and rovers delivered to the planet's surface. The development of Martian missions originates from the 1960s [1], when it launched a series of spacecraft to planet Mars. The most interesting of Marian's missions, from the point of view of working out landing schemes, are the following: Viking 1, Viking 2, Pathfinder, Spirit, Opportunity, Phoenix and Curiosity. In continuation of these Martian missions, a joint "ExoMars" mission is being implemented between the Federal Space Agency (Roscosmos) and the European Space Agency (ESA). This mission consists of two stages. In 2016 launched the first stage of mission ExoMars, including the satellite TGO (Trace Gas Orbiter) with the scientific equipment and the descent module ESA Schiaparelli. Tasks of the descent module of the ESA Schiaparelli were to test the method a controlled landing using propulsion system. However, due to errors in the onboard computer, Schiaparelli crashed on the surface of Mars. The second stage of the mission ExoMars was initially planned for 2018. Due to some difficulties, the development of the second stage was extended for two years. Launch to the Mars planet of the Russian "ExoMars" descent module with European rover is scheduled for 2020 [2].

Of particular interest is the develop of process of controlled landing of the lander on the surface of Mars. The process of controlled landing is accompanied by the appearance of negative effects (erosion of the Martian surface, lift loss, heat and power load) affecting the correct operation of the sensors, on-board systems and payloads as a result of interaction of the plumes of the propulsion system with the surface of Mars.

Despite the rarefied atmosphere of Mars, when performing the final stage of controlled landing of landing platform an effect of lift loss. The occurrence of this effect is well studied for aircraft vertical takeoff and landing. When the propulsion system is operating at a low altitude (the moment of takeoff and landing), the air recirculation

Prospects of Fundamental Sciences Development (PFSD-2017)
AIP Conf. Proc. 1899, 060010-1–060010-7; https://doi.org/10.1063/1.5009881
Published by AIP Publishing. 978-0-7354-1587-4/$30.00

effect occurs in the bottom region of the aircraft, because of which a region of reduced pressure may appear in it, resulting in a lift loss effect. Value of effect lift loss is expressed by the following ratio [3-9]:

$$L_f = \frac{G - G_0}{P}, \tag{1}$$

where G and G_0 – the integrals of the pressure forces on the bottom surface of the craft, N; P – the thrust of propulsion system, N.

Value G is calculated by integrating utilization pressure area of the bottom of the craft at altitude h when operating propulsion system with thrust P. Value G_0 is determined in a similar way under the condition $h \to \infty$.

Previously, the study of lift loss effect in the conditions of Mars and other planets were not carried out. In this regard, it is necessary to study the influence of lift loss effect on the controlled landing of “ExoMars” landing platform in Mars conditions. In the case of a lift loss, it may be necessary to adjust the control algorithm and include additional power to compensate for the thrust loss.

The aim of this work is a numerical study of the impingement of adjacent and multiple plumes consisting of four supersonic plumes with the Martian surface at the final stage a controlled landing “ExoMars” landing platform at a altitude from 1 to 0.3 meters and to investigate the ground effect lift loss in the conditions of Mars.

PHYSICAL AND MATHEMATICAL MODEL

The final stage of controlled landing of “ExoMars” landing platform is considered. A simplified sketch configuration of the landing module is shown in Figure 1 [10]. Concluding braking is at altitude less than 10 meters, then the propulsion system operates with a capacity that provides a vertical descent speed of the lander 1.8-2 m/s [11]. Towards the surface of Mars, shutting down the propulsion system is performed by the signal of touch sensors installed at each boarding leg. This is followed by purging of the cavities of the chambers to displace the fuel from the inlet to the chambers of the pipes and cavities of the cells [12].

The surface of the landing area was set uneven, with a slope angle of 15 degrees (Fig.1c). The altitude of the position of the landing platform from the cut of the engine nozzle to the surface in the range from 1 to 0.3 meters was varied. Studies have shown that a significant effect of plumes have at altitude below 1 meter. Two mode of propulsion system are considered, at maximum mode, the thrust is 13734 N, and at minimum mode, the thrust is 1962 N [12].

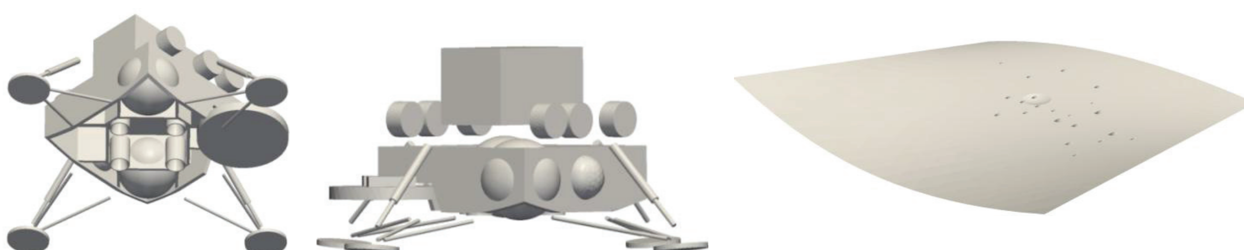

(a) (b) (c)

FIGURE 1. Conceptual design of “ExoMars” landing platform (a), (b) and landing surface (c)

For the mathematical description of the impingement of plumes with the landing site surface, the turbulent flow of a viscous compressible gas in the three-dimensional approximation is considered [13-19]. The system of equations in a rectangular Cartesian coordinate system x_1, x_2, x_3 for nonstationary gas flow has the form:

The continuity equation:

$$\frac{\partial \rho}{\partial t} + \frac{\partial}{\partial x_j}\left[\rho u_j\right] = 0, \tag{2}$$

where ρ – density, kg/m^3; t – time, s; u_j – velocity, m/s; x_j – coordinate, m.

The momentum equation:

$$\frac{\partial}{\partial t}(\rho u_i)+\frac{\partial}{\partial x_j}\left[\rho u_i u_j + p\delta_{ij} - \tau_{ji}\right]=0, \quad (3)$$

where p – pressure, Pa; δ_{ij} – Kronecker delta.

The viscous stress tensor has the following form:

$$\tau_{ij} = 2\mu\left[\frac{1}{2}\left(\frac{\partial u_i}{\partial x_j}+\frac{\partial u_j}{\partial x_i}\right)-\frac{1}{3}\frac{\partial u_k}{\partial x_k}\delta_{ij}\right], \quad (4)$$

The energy equation:

$$\frac{\partial}{\partial t}(\rho E)+\frac{\partial}{\partial x_j}\left[\rho u_j E + u_j p + q_j - u_i\tau_{ij}\right]=0, \quad (5)$$

where E – the total internal energy, J; q_j – heat-flux, J/(m^2·s).

The ideal gas equation:

$$p = \rho RT, \quad (6)$$

where T – temperature, K; R – gas constant, J/(kg·K), indexes $i,\ j,\ k = 1,\ 2,\ 3$.

To close the system of equations (2)-(6) Menter's $SST\ k-\omega$ turbulent model is used [20].

At the initial moment of time the temperature and pressure environment of Mars was set to 250 K and 650 Pa, the velocity in the completely computational domain was equal to zero. At the inlet of the nozzles of propulsion system engines a uniform subsonic gas flow was assumed with velocity, temperature and pressure of the combustion chamber. On the outer boundaries of the computational domain, "soft" boundary conditions were used.

To implement the physical and mathematical model and conduct numerical research was used free software OpenFOAM [21]. Numerical method is based on finite volume method. Numerical mesh was generated using NetGen algorithm. A difference scheme of MUSCL-Hancock type TVD of the second order of accuracy was used [22]. From the approximate solution of the Riemann problem according to the HLLC scheme, there were fluxes through the faces of the computational grid cells. System of linear of algebraic equations was solved using the Gauss-Seidel method. The time sampling was carried out by a four-step Runge-Kutta method of second-order accuracy. Numerical investigation were done using SKIF Cyberia supercomputer of Tomsk State University.

Validation of the calculations results was performed by the examination of the spatial convergence of a simulation and the comparison of numerical results with theoretical and experimental data of other authors. The results of numerical calculations of the impingement of a single plume with surfaces with experimental data [9] for the ground effect lift loss are compared. Schematic of the experimental setup [9] is shown on Figure 2.

Experimental setup [9] consist of canonical nozzle ($\Gamma 1$) with throat diameter $d_* = 0.0254$ meter and exit diameter $d = 0.0275$ meter ($\Gamma 4$), disk ($\Gamma 3$) mounted at the exit nozzle with diameter $D = 0.254$ meter. Distance from the nozzle exit with disk to plate ($\Gamma 5$) in the experiments [9] ranged from $h/d = 1.84$ to $h/d = 9.23$. As the working fluid used air. The experiment was conducted under the following initial conditions: the temperature of the air in the cylinders and the environment was equal to 293.15 K. The pressure ratio in the inlet nozzle ($\Gamma 1$) to the ambient pressure in the experiments corresponded to $p_0/p_a = 3.7$ and $p_0/p_a = 5$. Velocity of gas flow at exit nozzle was 1.5 Mach number.

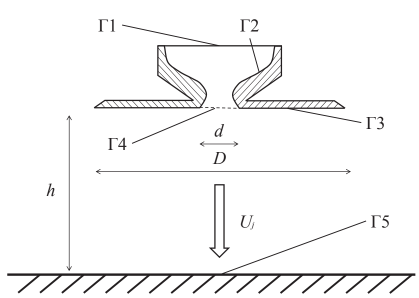

FIGURE 2. Schematic of the experimental setup [9]

For distance $h/d = 1.84$ using the developed method of calculation, has been conducted research on grid convergence. In the calculations varied the number of cells on the cut along the exit radius of the nozzle $\Gamma 4$ with the implementation of conditions for the preservation of cell size in the whole computational domain. Then the value G at the boundary $\Gamma 3$ was calculated for a stationary distribution of the gas parameters. Figure 3 shows a graph of the magnitude of the power of influence of the peripheral flow of the plume on the solid wall $\Gamma 3$ depending on the number of cells along the exit radius at the nozzle $\Gamma 4$. As can be seen from the graph the optimum size of the cells is the computational domain with 35 cells on the radius of the nozzle exit, the size of a side of the cell in this variant is 0.0004 meters.

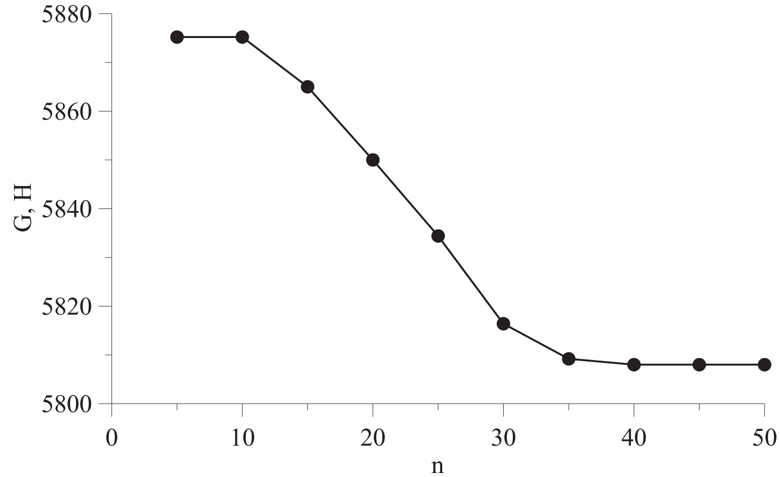

FIGURE 3. The value of the force influence of the plume on the wall $\Gamma 3$ depending on the number of cells along the exit radius of nozzle $\Gamma 4$

Comparison of numerical results and experimental data [9] of ground effect lift loss for pressure ratio $p_0 / p_a = 3.7$ and plate distances $h/d = 1.84 \div 9.23$ is shown on Figure 4. It can be seen that a good agreement has been obtained between numerical calculations and experimental data [9].

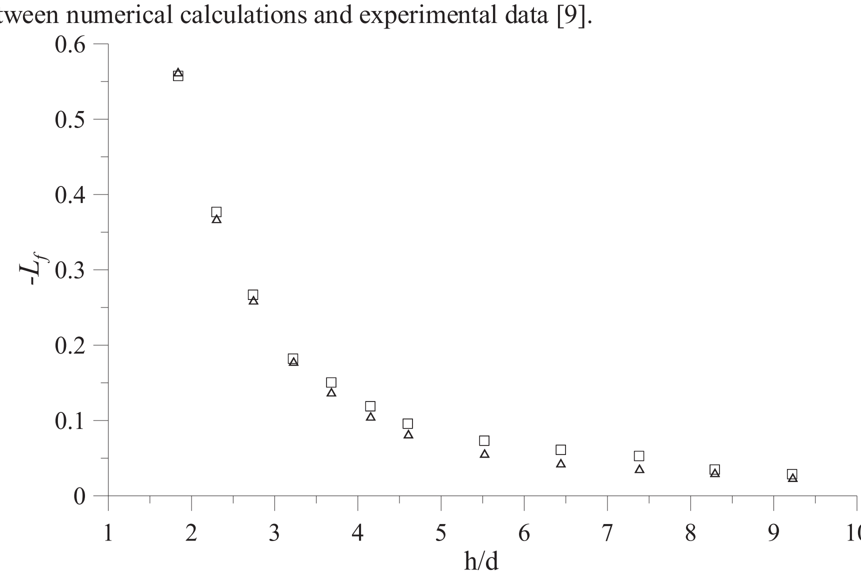

FIGURE 4. Comparison numerical results and experimental data for ground effect lift loss [9]
(□ - numerical results, Δ - experimental data)

NUMERICAL RESULTS

According to the results of numerical studies of the final stage of controlled landing "ExoMars" landing platform, the distribution of parameters of gas in the area of lander in the result of impingement of adjacent and multiple plumes with surface of Mars was obtained for minimum and maximum thrust of propulsion system and the location of the landing platform at an altitude of 1, 0.5 and 0.3 meters. Figure 5 shows the isosurfaces of Mach numbers at the time 0.3 seconds of operation of propulsion system depending on the altitude and thrust. When propulsion system works at the minimum thrust, the plumes have mutual influence, which affects the form of each plume. At maximum thrust, when the location of the landing platform at an altitude of 1 meter plumes are merged into adjacent plume. With further decrease of altitude of landing platform adjacent plume separated into four plumes forming it. At maximum thrust, a much stronger mutual influence is noticeable, in contrast to the operation of the propulsion system at minimum thrust.

To determine the ground effect lift loss was carried out the integration of the pressure forces applied to the bottom of the landing platform. Figure 6 shows the results on the distribution of the pressure field on the bottom surface of the landing platform. Table 1 shows the values of the resulting forces on the bottom landing platform and the calculation of lift loss in Mars environment.

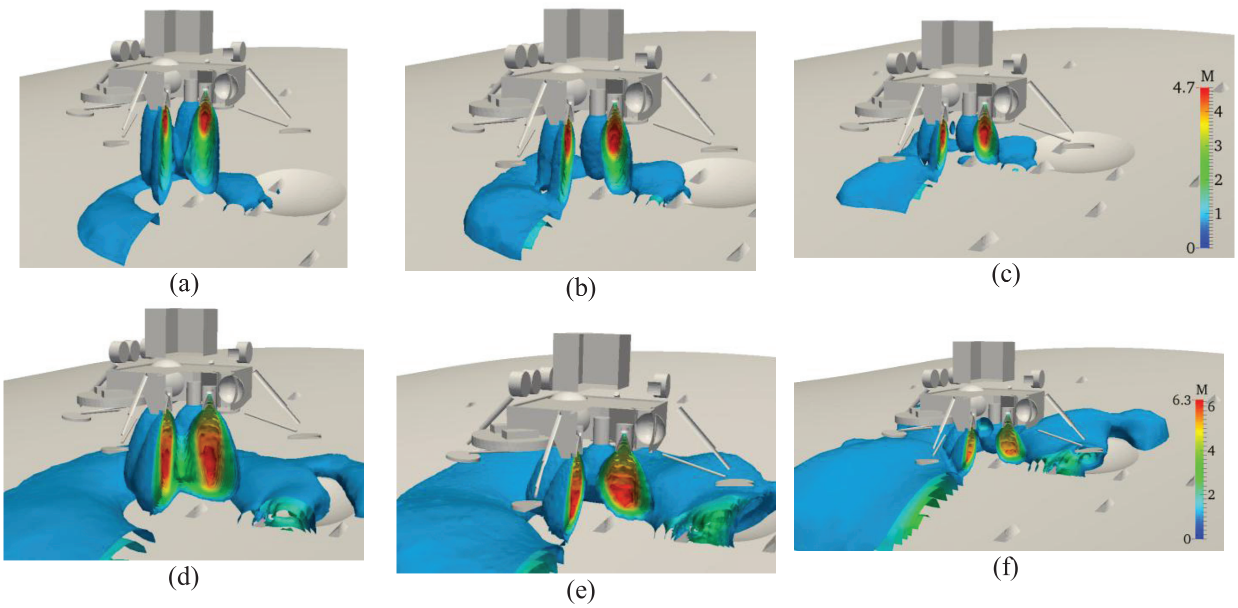

FIGURE 5. Isosurfaces of Mach numbers: minimum thrust at altitude 1 meter (a), minimum thrust at altitude 0.5 meter (b), minimum thrust at altitude 0.3 meter (c), maximum thrust at altitude 1 meter (d), maximum thrust at altitude 0.5 meter (e), maximum thrust at altitude 0.3 meter (f)

TABLE 1. The results of calculations of the plumes force impact on the bottom of landing platform and lift loss.

	Level of propulsion system thrust					
	Minimum			**Maximum**		
G_0, N	1521			1466		
Altitude, m	1	0.5	0.3	1	0.5	0.3
G, N	1488	1700	1879	1068	2132	5166
$G-G_0$, N	-33	179	358	-389	666	3700
L_f	-0.0165	0.0895	0.179	-0.0272	0.0465	0.258

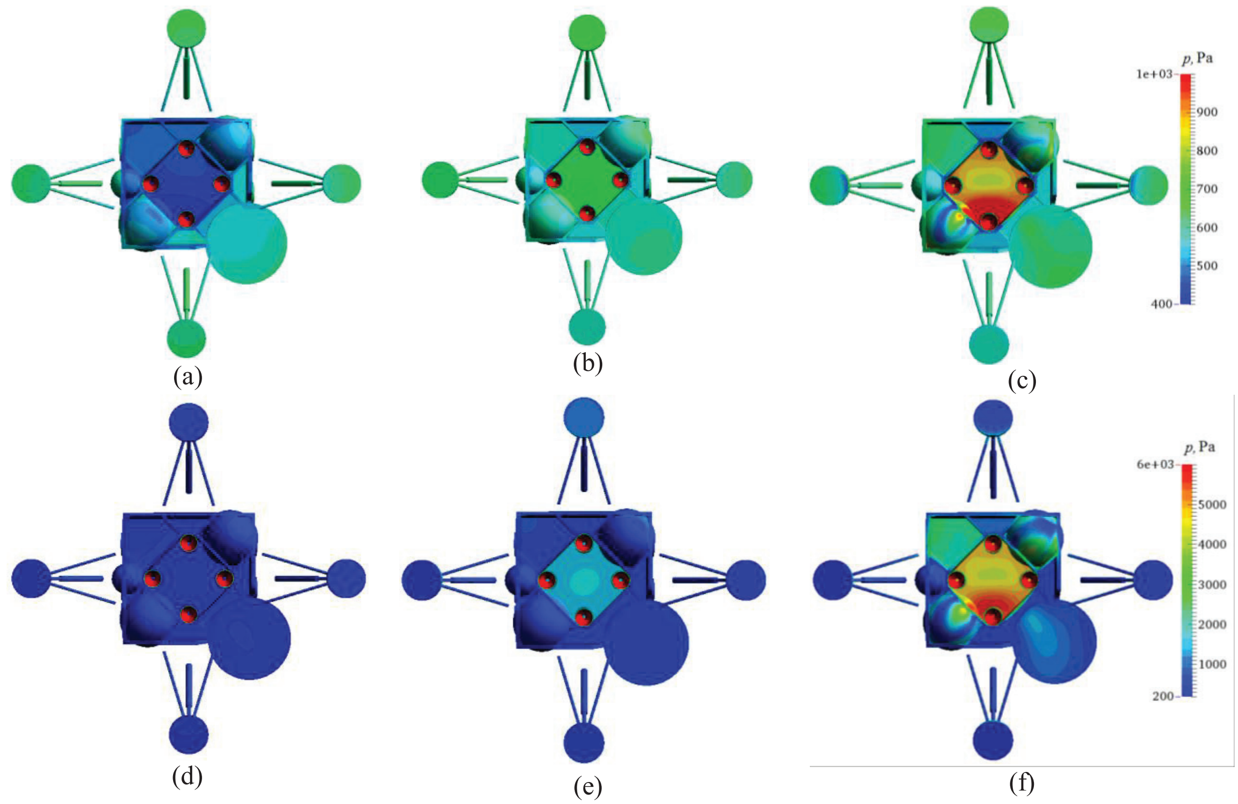

FIGURE 6. Distribution of pressure field on the bottom surface of landing platform (minimum thrust at altitude 1 meter (a), minimum thrust at altitude 0.5 meter (b), minimum thrust at altitude 0.3 meter (c), maximum thrust at altitude 1 meter (d), maximum thrust at altitude 0.5 meter (e), maximum thrust at altitude 0.3 meter (f)).

The ground effect lift loss is observed only at altitude of 1 meter. At the minimum thrust, the lift loss value is 1.6%, and at the maximum thrust 2.7% of the total thrust of the propulsion system. With a decrease altitude of landing platform from 1 meter to 0.3 meters, the pressure in the bottom region at the minimum thrust of propulsion system increases to 1 kPa, and at the maximum to 6 kPa. The ground effect lift loss disappears and adds a positive force of external pressure on the bottom surface of landing platform. From altitude of 0.5 meters to 0.3 meters, the external force increases with a minimum thrust from 9% to 18%, and at maximum thrust from 5% to 26% of the total thrust of the propulsion system.

CONCLUSION

Numerical study of the ground effect lift loss in Mars environment for "ExoMars" landing platform configuration have shown that the effect at altitude 1 meter regardless of the thrust of propulsion system does not exceed 2.7% of the level of thrust or 389 N. Analysis of the results shows that the lift loss effect is insignificant. This follows from the fact that these values do not exceed the installed power of one engine of propulsion system for the measurement error and the maximum thrust tolerance. With a further altitude decrease of landing platform from 1 to 0.3 meter, a reverse external force is obtained, which can reach 3.7 kN when the propulsion system operates at maximum thrust.

ACKNOWLEDGMENTS

The work executed at financial support of the Ministry of education and science of the Russian Federation in the framework of the state assignment, project No 9.9063.2017/BCh.

REFERENCES

1. NASA (2017). Mars Planet Facts News & Images | NASA Mars rover + mission info. [online] Available at: https://mars.nasa.gov/ [Accessed 15 May 2017].
2. NPO im. S. A. Lavochkina. (2017). ExoMars-2020. [online] Available at: https://www.laspace.ru/projects/planets/exomars/ [Accessed 15 May 2017].
3. L. A. Wyatt, Aeronaut. Res. Council Rep. Memor. **749**, 1–38 (1964).
4. K. T. Yen, Report No. NADC-80057-60 (1980).
5. J. Louise and F. L. Marshall, J. Aircraft. **13,** 123–127 (1976).
6. Z. Xin and N. Dan Ing, J. Aircraft. **31,** 256–262 (1994).
7. D. B. Levin and D. A. Wardwell, J. Aircraft **34,** 400–407 (1997).
8. I. M. Chotapalli, A. Krothapalli, M. B. Alkislar, and L. M. Lourenco, AIAA J **45**, 793–805 (2007).
9. A. Krothapalli, E. Rajkuperan, and F. Alvi, L. Lourence, J. Fluid Mech. **392**, 155–181 (1999).
10. V. V. Khartov, M. B. Martynov, A. V. Lukiyanchikov, and S. N. Alexashkin, VESTNIK NPO named after S.A. Lavochkin **23**, 5–12 (2014).
11. V. N. Likhachev and V. P. Fedotov, VESTNIK NPO named after S.A. Lavochkin **23**, 58–64 (2014).
12. L. G. Alexandrov, V. I. Morozov, S. S. Stepanov, A. A. Krylov, O. A. Kuzmin, A. V. Fedotov, and M. V. Maltsev, VESTNIK NPO named after S.A. Lavochkin **23**, 116–120 (2014).
13. L. G. Loytzyansky, *Mechanics of Liquid and Gas* (Drofa, Moscow, 2003) p. 840.
14. G. N. Abramovich, *Applied Gas Dynamics* (Nauka, Moscow, 1991) p. 600.
15. V. E. Alemasov, A. F. Dregalin, and A. P. Tishin, *The Theory of Rocket Engines* (Mashinostroenie, Moscow, 1980) p. 534.
16. V. N. Glaznev, V. I. Zapryagaev, and V. N. Uskov, *Jet and Nonstationary Flows in Gas Dynamics* (Siberian Branch of Russian Academy of Sciences, Novosibirsk, 2000) p. 200.
17. I. M. Vasenin, A. Y. Krainov, A. M. Lipanov, and E. R. Shrager, Comp. Math. Math. Phys+. **55**, 883–890 (2015).
18. I. M. Vasenin, V. L. Goiko, A. Y. Krainov, A. M. Lipanov, and E. R. Shrager, Russ. Phys. J. **57**, 1405–1411 (2015).
19. A. A. Glazunov, V. D. Goldin, V. G. Zverev, S. N. Ustinov, V. S. Finchenko, Thermophys. Aeromechan. **20**, 195–209 (2013).
20. F. R. Menter, AIAA J, **32**, 1598–1605 (1994).
21. The OpenFOAM Foundation. OpenFOAM User Guide and Programming Guide [online] Available at: http://openfoam.org [Accessed 15 May 2017].
22. E. F. Toro, *Riemann Solvers and Numerical Methods for Fluid Dynamics* (Springer-Verlag, Berlin, 2009) p. 724.